Available online at www.sciencedirect.com

SCIENCE DIRECT

Virology 330 (2004) 447–459

VIROLOGY

www.elsevier.com/locate/yviro

A complex of seven vaccinia virus proteins conserved in all chordopoxviruses is required for the association of membranes and viroplasm to form immature virions

Patricia Szajner[a], Howard Jaffe[b], Andrea S. Weisberg[a], Bernard Moss[a,*]

[a]*Laboratory of Viral Diseases, National Institute of Allergy and Infectious Diseases, National Institutes of Health, Bethesda, MD 20892, United States*
[b]*Protein/Peptide Sequence Facility, National Institute of Neurological Disorders and Stroke, National Institutes of Health, Bethesda, MD 20892, United States*

Received 17 August 2004; returned to author for revision 28 September 2004; accepted 5 October 2004
Available online 28 October 2004

Abstract

Early events in vaccinia virus (VAC) morphogenesis, particularly the formation of viral membranes and their association with viroplasm, are poorly understood. Recently, we showed that repression of A30 or G7 expression results in the accumulation of normal viral membranes that form empty-looking immature virions (IV), which are separated from large masses of electron-dense viroplasm. In addition, A30 and G7 physically and functionally interact with each other and with the F10 protein kinase. To identify other proteins involved in early morphogenesis, proteins from cells that had been infected with vaccinia virus expressing an epitope-tagged copy of F10 were purified by immunoaffinity chromatography and analyzed by gel electrophoresis. In addition to F10, A30, and G7, viral proteins A15, D2, D3, and J1 were identified by mass spectrometry of tryptic peptides. Further evidence for the complex was obtained by immunopurification of proteins associated with epitope-tagged A15, D2, and D3. The previously unstudied A15, like other proteins in the complex, was expressed late in infection, associated with virus cores, and required for the stability and kinase activity of F10. Biochemical and electron microscopic analyses indicated that mutants in which A15 or D2 expression was regulated by the *Escherichia coli lac* operator system exhibited phenotypes characterized by the presence of large numbers of empty immature virions, similar to the results obtained with inducible A30 and G7 mutants. Empty immature virions were also seen by electron microscopy of cells infected with temperature-sensitive mutants of D2 or D3, though the numbers of membrane forms were reduced perhaps due to additional effects of high temperature.
Published by Elsevier Inc.

Keywords: Chordopoxviruses; Vaccinia virus proteins; Immature virions

Introduction

Vaccinia virus (VAC) morphogenesis occurs in the cytoplasm of infected cells through a series of intermediate structures that have been visualized by electron microscopy (Dales and Siminovitch, 1961; Grimley et al., 1970; Risco et al., 2002). Crescent-shaped membranes with electron-dense granular material (viroplasm) adjacent to the concave side evolve into spherical, immature virions (IV), which enclose a nucleoprotein mass. Further maturational events, including proteolytic processing of viral core proteins (Ansarah-Sobrinho and Moss, 2004; Byrd et al., 2003; Moss and Rosenblum, 1973) and intramolecular disulfide bonding of viral membrane proteins (Senkevich et al., 2002), result in the transformation of IV into infectious brick-shaped intracellular mature virions (IMVs). Some IMVs are wrapped by cisternae, derived from the *trans*-Golgi network or early endosomes (Hiller and Weber, 1985; Schmelz et al., 1994; Tooze et al., 1993) to form intracellular enveloped virions (IEVs). The IEVs, which contain two additional membranes relative to IMV, bind to microtubules and are transported to the periphery of the cell (Geada et al., 2001; Hollinshead

* Corresponding author. Laboratory of Viral Diseases, National Institutes of Health, 4 Center Drive, MSC 0445, Bethesda, MD 20892-0445. Fax: +1 301 480 1147.
E-mail address: bmoss@nih.gov (B. Moss).

0042-6822/$ - see front matter. Published by Elsevier Inc.
doi:10.1016/j.virol.2004.10.008

et al., 2001; Rietdorf et al., 2001; Ward and Moss, 2001a, 2001b; Ward and Moss, 2004), where the outermost membrane fuses with the plasma membrane, depositing cell-associated enveloped virions (CEVs) on the cell surface (Blasco and Moss, 1992). Actin polymerizes at the site of membrane fusion resulting in the formation of microvilli with CEV at their tips, thereby facilitating virus spread (Hollinshead et al., 2001; Rietdorf et al., 2001; Stokes, 1976; Ward and Moss, 2001a). Some extracellular enveloped virions (EEVs) are released into the medium and promote spread to distant cells (Appleyard et al., 1971; Blasco et al., 1993; Boulter and Appleyard, 1973; Payne, 1980).

Early events in VAC morphogenesis, particularly the formation of viral membranes and their association with the viroplasm, are poorly understood. Recently, we showed that the viral A30 and G7 proteins are components of the virus core and that repression of either gene results in the accumulation of normal-looking viral membranes forming empty-looking IVs that are separated from large masses of viroplasm (Szajner et al., 2001b, 2003). A30 and G7 interact with each other, and this association is necessary for the stability of each protein. In addition, when either A30 or G7 is repressed, phosphorylation of the A17 membrane protein by the F10 kinase is severely reduced (Szajner et al., 2004b). This observation led us to find a physical interaction of A30 and G7 with F10 (Szajner et al., 2004b). Just as A30 and G7 are mutually dependent on each other for stability, F10 is nearly undetectable in the absence of A30 and G7. Furthermore, phosphorylation of A30 is dependent on the F10 kinase and autophosphorylation of F10 is stimulated by A30 and G7. F10 is also required for viral membrane formation (Traktman et al., 1995; Wang and Shuman, 1995) and the catalytic site is required for this function but not for the physical interaction with A30 and G7 (Szajner et al., 2004a, 2004b). Thus, F10 may have distinct roles in the formation of the viral membrane and the association of the membrane with viroplasm.

Using epitope tagging, immunoaffinity purification, and mass spectrometry, we now show that A15, D2, D3, and J1 are components of the complex containing A30, G7, and F10. Previously isolated viruses with conditionally lethal mutations of J1 (Chiu and Chang, 2002), D2 (Dyster and Niles, 1991), and D3 (Dyster and Niles, 1991) have been directly or indirectly shown to have blocks in morphogenesis. Our present study, which includes the initial characterization of A15 and a further characterization of D2 and D3, demonstrates that these proteins are also required for the association of membranes and viroplasm.

Results

Identification of a complex containing seven VAC proteins

In previous studies we provided evidence for a complex containing A30, G7, and F10 proteins (Szajner et al., 2003, 2004b). Sodium dodecyl sulfate-polyacrylamide gel electrophoresis (SDS-PAGE) of metabolically labeled proteins, however, suggested that additional polypeptides co-immunoprecipitated with F10. To identify additional interacting proteins, extracts from cells infected with vF10V5 (previously called vWT-F10V5), a recombinant VAC that contains a V5 epitope-tagged copy of F10 (Szajner et al., 2004b), were incubated with an anti-V5 monoclonal antibody (MAb) covalently linked to beads. After washing, the bound proteins were eluted, resolved by SDS-PAGE, and visualized by Coomassie blue staining. As a control, extracts from cells infected with wild-type VAC were analyzed in parallel. By comparison of the bands in the two lanes, we could discriminate between proteins that bound nonspecifically to the beads from those that were associated with F10V5. Five distinct bands unique to the sample from cells infected with F10V5 were detected (Fig. 1). These bands were excised, digested with trypsin, and analyzed by liquid chromatography and mass spectrometry. Bands of about 50, 42, and 9 kDa contained peptides with masses corresponding to predicted ones from the F10, G7, and A30 proteins, respectively. Additional tryptic peptides from the bands indicated in Fig. 1 were identified as digestion products of A15, D2, D3, and J1.

The proteins that co-purified with F10V5 could represent individual proteins bound to F10, multiple small complexes, or a single large complex. The existence of complexes was previously shown by co-purification of F10, A30, and G7 when antibodies to epitope-tagged F10 or A30 were used (Szajner et al., 2004b). To extend the analysis, we made the recombinant virus vA15V5, in which a V5 epitope tag was appended to the predicted C-terminus of the A15L open reading frame (ORF) without disturbing its natural promoter. To facilitate isolation of the recombinant virus, the ORF for enhanced green fluorescent protein (GFP) regu-

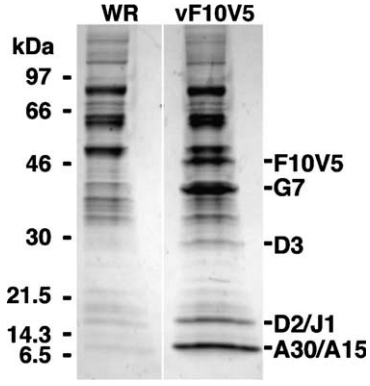

Fig. 1. Identification by mass spectrometry of viral proteins that associate with affinity purified F10V5. BS-C-1 cells were infected with vF10V5 or VAC strain WR for 48 h. The cells were lysed and clarified cell lysates were incubated with anti-V5 MAb conjugated to beads. After washing, proteins bound to the beads were eluted, resolved by SDS-PAGE, and stained with Coomassie blue. The positions and masses of marker proteins are shown on the left. The bands indicated on the right were excised and the proteins were identified by liquid chromatography and mass spectroscopy of tryptic peptides.

lated by the VAC P11 promoter was co-inserted between the A15L and A14L ORFs with the deletion of the non-essential A14.5 gene (Betakova et al., 2000). Cells were infected with vA15V5 and the proteins present in the total lysate or the ones affinity purified with anti-V5 MAb were analyzed by Western blotting with antibodies specific for F10, G7, J1, V5, and A30. Strips excised from the Western blots are shown in Fig. 2A. The bands detected in the total lysates of cells infected with the control virus (vT7lacOI) or vA15V5 were identical, except for the expected absence of the epitope-tagged A15V5 in the former. Each of the proteins

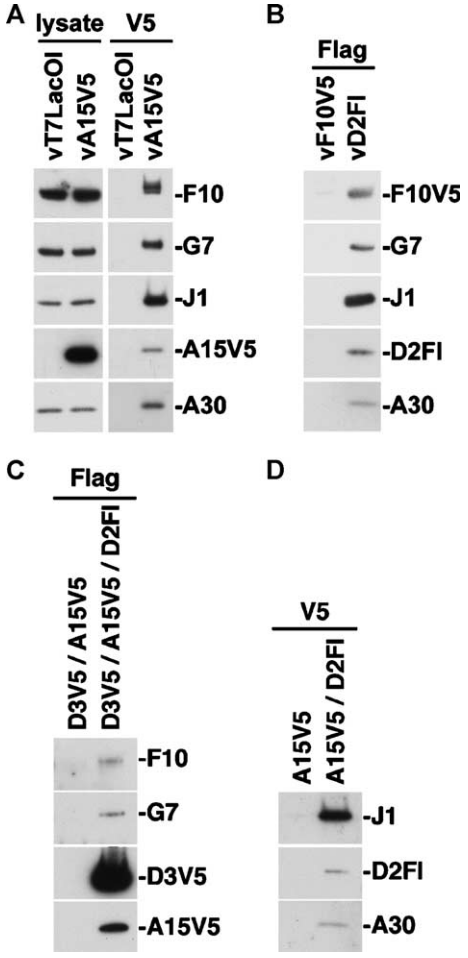

Fig. 2. Identification of viral protein components of the complex by Western blotting. (A) Western blots of proteins that co-purified with A15V5. BS-C-1 cells were infected for 24 h with vA15V5 or control virus vT7lacOI and the clarified lysates were incubated with beads containing covalently bound anti-V5 MAb and then washed extensively. The lysate and the proteins bound to the V5 MAb were analyzed by SDS-PAGE, transferred to a nylon membrane, and probed with antibodies to F10, G7, J1, V5, and A30. (B) Western blots of proteins that co-purified with D2Fl. Similar to panel A except that cells were infected with vD2Fl or the parental vF10V5 and the proteins were purified by binding to beads containing covalently bound anti-Flag MAb. (C and D) Western blotting following co-transfections. Cells were infected with vT7lacOI and transfected with combinations of plasmids expressing D3V5, A15V5, and D2Fl. Proteins were immunopurified using beads containing covalently linked anti-Flag MAb (C) or anti-V5 MAb (D) and analyzed by SDS-PAGE followed by Western blotting with antibodies to the proteins indicated on the right.

detected in the total lysate of cells infected with vA15V5 was also detected in the affinity-purified complex from these cells, whereas none of these proteins were detected in the affinity-purified material from cells infected with control virus (Fig. 2A). These experiments supported the existence of a complex containing A15, F10, G7, J1, and A30.

To provide further evidence for the presence of D2 in the complex, we made recombinant VAC vD2Fl with a Flag-tag appended to the predicted C-terminus of the D2L ORF in vF10V5, again without disturbing the D2 promoter and using GFP as a reporter. Although referred to as vD2Fl, this recombinant has a V5 tag on F10 as well as a Flag tag on D2. Proteins from cells infected with vD2Fl or the parental vF10V5 were immunopurified with anti-Flag antibody and analyzed by Western blotting with specific antibodies. F10V5, G7, J1, D2Fl, and A30 were each detected in the affinity purified proteins from cells infected with vD2Fl but not from the similarly purified proteins from cells infected with control virus (Fig. 2B).

Because of overlapping ORFs and transcriptional signals, we did not make a recombinant virus with an epitope-tagged D3. Instead, we used a transfection expression protocol. Cells were infected with vTF7-3, a recombinant virus that constitutively expresses the bacteriophage T7 RNA polymerase (Fuerst et al., 1986), and transfected with various combinations of plasmids containing a V5-tagged copy of A15 (A15V5), a V5-tagged copy of D3 (D3V5), or a Flag-tagged copy of D2 (D2Fl), each under the control of the T7 promoter. Extracts of cells that had been transfected with plasmids expressing A15V5 and D3V5 in the presence or absence of a plasmid expressing D2Fl were incubated with an anti-Flag MAb conjugated to beads. The bound proteins were analyzed by SDS-PAGE followed by Western blotting. F10, G7, D3V5, and A15V5 were detected only when D2Fl was expressed (Fig. 2C). Using a similar transfection approach, J1, D2Fl, and A30 were shown to be associated with A15V5 (Fig. 2D). Taking the experiments in this section together, we concluded that A15, A30, D2, D3, F10, G7, and J1 are part of a multiprotein complex, though subcomplexes may also exist.

To further characterize the complex, we used a mixture of [^{35}S]methionine and [^{35}S]cysteine to metabolically label proteins in cells infected with vA15V5 or wild-type VAC strain WR. Infected cell extracts were incubated with beads covalently linked to anti-V5 MAb and the bound proteins were analyzed by SDS-PAGE and visualized by autoradiography. Bands specific for the extracts from cells infected with the vA15V5, relative to the control, had apparent masses of 42, 27, 18 (doublet), 12, and 9 kDa, consistent with G7, D3, J1 and D2, A15V5, and A30 proteins, respectively (Fig. 3). Except for the absence of a radioactive 50-kDa band, this pattern was similar to the Coomassie blue-stained bands obtained by affinity purification of proteins associated with F10V5 (Fig. 1) and no additional bands were detected. Western blotting or mass spectrometry confirmed the identities of G7, D3, J1, A15V5, and A30 (data not shown). Since the

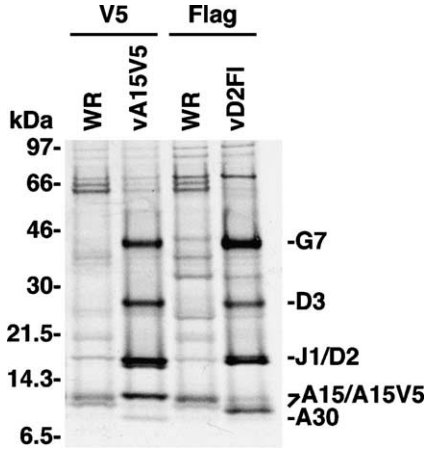

Fig. 3. Autoradiographs of metabolically labeled proteins that co-purified with A15V5 or D2Fl. BS-C-1 cells were infected with vA15V5, vD2Fl, or control VAC WR, and labeled with a [^{35}S]methionine and [^{35}S]cysteine mixture from 7 to 24 h after infection. The cells were lysed and the clarified extracts were incubated with beads containing covalently bound anti-V5 or -FLAG MAb as indicated at the top. After washing, the proteins were eluted with SDS sample buffer and analyzed by SDS-PAGE followed by autoradiography. The masses (kDa) of marker proteins are indicated on the left. Viral proteins with mobilities that correspond to bands not present in the control gel are indicated on the right.

upper band of the 18-kDa doublet was identified by Western blotting as the J1 protein, the lower band corresponds to the D2 protein. Assuming a complex with a single subunit of each protein, one would expect the autoradiographic intensities to follow the amount of cysteine and methionine, that is, G7 > F10 > D3 > J1 > A15, D2 > A30. Except for F10, the results were generally in accord with this ranking. Thus, G7, D3, and J1 were the most intense, D2 and A15 were intermediate, and A30 was the least intense. J1 was reported to self-interact by yeast two-hybrid analysis (McCraith et al., 2000), and the higher intensity of J1 compared to D3 suggests the presence of two copies. The extreme weakness of the radioactive band corresponding to A30 was expected, since this protein is predicted to have a single methionine at the initial position and no cysteines. The absence of a 50-kDa band corresponding to F10 could not be explained by a simple deficiency of cysteines and methionine residues.

A similar experiment was carried out by infecting cells with vD2Fl and labeling with a mixture of [^{35}S]methionine and [^{35}S]cysteine. Cell extracts were incubated with beads conjugated to an anti-Flag MAb and analyzed by SDS-PAGE and visualized by autoradiography. The pattern was similar to that obtained in the previous experiment with some minor differences (Fig. 3). D2Fl was identified by Western blotting as the upper band of the 18-kDa doublet, consistent with the added mass of the Flag tag, and J1 was the lower band. In addition, the 12-kDa A15V5 in the previous experiment was replaced by a 10-kDa A15 without the epitope tag. The A30 band, which was faint in the previous experiment, was barely detected. Again, we did not see a labeled F10 band. Similarly, ^{35}S-labeled F10 was not detected when proteins associated with A30 were analyzed (Szajner et al., 2004b). It is clear from both mass spectrometry and Western blotting experiments that F10 is a component of the protein complex. We are unsure of whether the long labeling time in amino acid-deficient medium is causing anomalous results, perhaps due to a more rapid turnover of F10 compared to the other proteins, or whether F10 is present in a subset of complexes.

A15 is a late protein associated with the virus core

The previously studied components of the complex, namely A30, D2, D3, F10, and G7, are expressed late in infection. Examination of the DNA upstream of the A15L ORF revealed a typical TAAAT late promoter motif. vA15V5 was used to experimentally determine the time of A15V5 synthesis since the promoter of the A15 ORF had not been modified. The expected band with an apparent mass of 12 kDa was detected by SDS-PAGE and Western blotting with anti-V5 MAb at 6 h after infection and increased in intensity during the remainder of the 24-h time course (Fig. 4A). The A15V5 protein was not detected in lysates of cells infected in the presence of the DNA synthesis inhibitor cytosine arabinoside (AraC) (Fig. 4A). The promoter sequence, time of synthesis, and inhibition by AraC indicated that a stringent late promoter regulates A15 expression.

The association of A15V5 with sucrose gradient-purified virions was demonstrated by Western blotting. Detergent extraction experiments were carried out to determine whether A15V5 is located in the membrane or core fraction of virions. Purified IMVs were treated with the nonionic

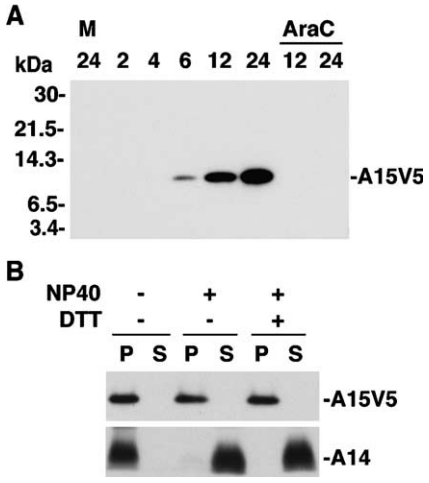

Fig. 4. Synthesis of A15V5 and localization in virus particles. (A) Western blot analysis. BS-C-1 cells were mock infected (M) or infected with vA15V5 in the absence or presence of cytosine arabinoside (AraC) and harvested at 2–24 h postinfection as indicated. Total cell lysates were analyzed by SDS-PAGE and Western blotting with anti-V5 MAb. Masses (kDa) of marker proteins are indicated at the left. (B) Virion fractionation. IMVs were purified by sucrose gradient centrifugation from cells infected with vA15V5 and incubated in buffer containing (+) or lacking (−) NP-40 or DTT. The mixture was centrifuged and the proteins in the pellet (P) and supernatant (S) were analyzed by SDS-PAGE and Western blotting using anti-V5 and anti-A14 antibodies as indicated on the right.

detergent Nonidet P-40 (NP-40) with or without reducing agent and centrifuged to separate the detergent soluble (membrane) from the insoluble (core) fractions. The fractions were analyzed by SDS-PAGE and immunoblotting with anti-V5 MAb. A15V5 was detected exclusively in the detergent-insoluble fraction (Fig. 4B). As a control to demonstrate the extractability of a membrane protein, the blots were also probed with antibody to the A14 protein, which was completely released into the detergent-soluble membrane fraction (Fig. 4B). Thus A15, like A30, G7, F10, D2, and D3, is packaged in virus cores.

Core proteins are probably incorporated into virions at the time of IV formation. Electron microscopy was carried out to localize A15V5 in immature and mature virus particles. Thin sections of cells infected with vA15V5 were incubated with anti-V5 MAb followed by protein A conjugated to gold spheres. Although the labeling was relatively sparse, the majority of gold particles were associated with the electron-dense material within the IV and with the cores of the IMV (Fig. 5). Gold particles were not associated with viral structures in cells infected with wild-type virus lacking a V5 epitope tag, indicating the absence of significant background (data not shown).

Construction and characterization of recombinant viruses that inducibly express A15

We made three recombinant viruses in which A15 was regulated by the *E. coli lac* operator and bacteriophage T7 RNA polymerase and chose the most stringent one to investigate the role of the protein in virus replication. In each construct, vT7LacOI (Alexander et al., 1992), which contains an inducible copy of the T7 RNA polymerase and constitutively expresses *E. coli lac* repressor in the thymidine kinase locus, was used as the starting virus. Two steps were required to make vA15V5i, as described for the construction of other inducible viruses (Szajner et al., 2001b). First, a C-terminal V5-tagged copy of A15, regulated by a T7 promoter, *E. coli lac* operator, and the untranslated leader sequence of encephalomyocarditis virus RNA, was inserted into the hemagglutinin locus of vT7LacOI. Next, the endogenous A15 gene was deleted by homologous recombination using a plasmid encoding GFP under the control of a VAC late promoter. The recombinant virus v15V5i was isolated in the presence of IPTG and plaques were identified by the expression of GFP. We found, however, that small plaques formed in the absence of IPTG, indicating that either A15 was not absolutely required for virus replication or that expression of A15 was not stringently repressed in this construct. Thinking that the latter was more likely, we made two additional IPTG-inducible mutants that each had a V5 epitope-tagged copy of A15 under the control of the T7 promoter and *lac* operator, without the encephalomyocarditis leader, inserted directly into the endogenous A15L locus of vT7LacOI. In vA15V5Li, the IPTG-inducible A15V5 gene was in the original direction of the A15L ORF, while in the vA15V5Ri virus, the inducible gene was inserted in the reverse orientation (Fig. 6A). The gene encoding GFP, under the control of a VAC late promoter, was co-inserted to allow selection of the recombinant virus. Plaque formation was completely inhibited in the absence of IPTG in cells infected with vA15V5Ri (Fig. 6B), whereas small plaques formed with vA15V5Li (data not shown), suggesting that expression of A15V5 was more efficiently repressed in vA15V5Ri. We attribute the less stringent control in vA15V5Li to RNA originating from A16L and reading though the *lac* operator sequence. Presumably this read-through RNA can be inefficiently translated to produce low levels of A15V5, although this was not directly examined. In vA15V5Ri, the RNA originating from A16L is complementary to the A15V5 transcripts, which may partially suppress A15V5 expression as seen by the small plaque size relative to the parent virus vT7lacOI or vA15V5 even in the presence of IPTG (Fig. 6B). The overlap of A15V5 transcripts with A16L transcripts could also contribute to the slightly reduced plaque size in the presence of IPTG.

The inability of vA15V5Ri to form plaques in the absence of IPTG could be due to a reduction in virus spread or replication. To discriminate between these possibilities, we analyzed virus yields under one-step growth conditions. Initial experiments indicated that the yield of virus was proportionate to IPTG concentration, reaching a maximum

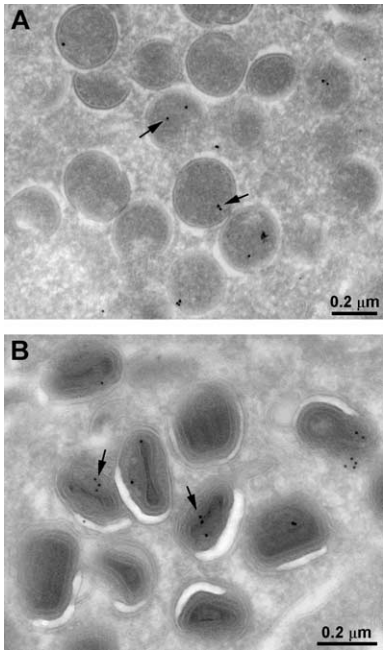

Fig. 5. Immunogold labeling of virus structures. BS-C-1 cells were infected with vA15V5 and harvested at 20 h after infection. The cells were fixed, frozen, sectioned, and incubated with an antiV5 MAb followed by protein A gold. The samples were viewed by transmission electron microscopy and representative fields containing IV (A) and IEV (B) are shown. Arrows point to representative gold grains.

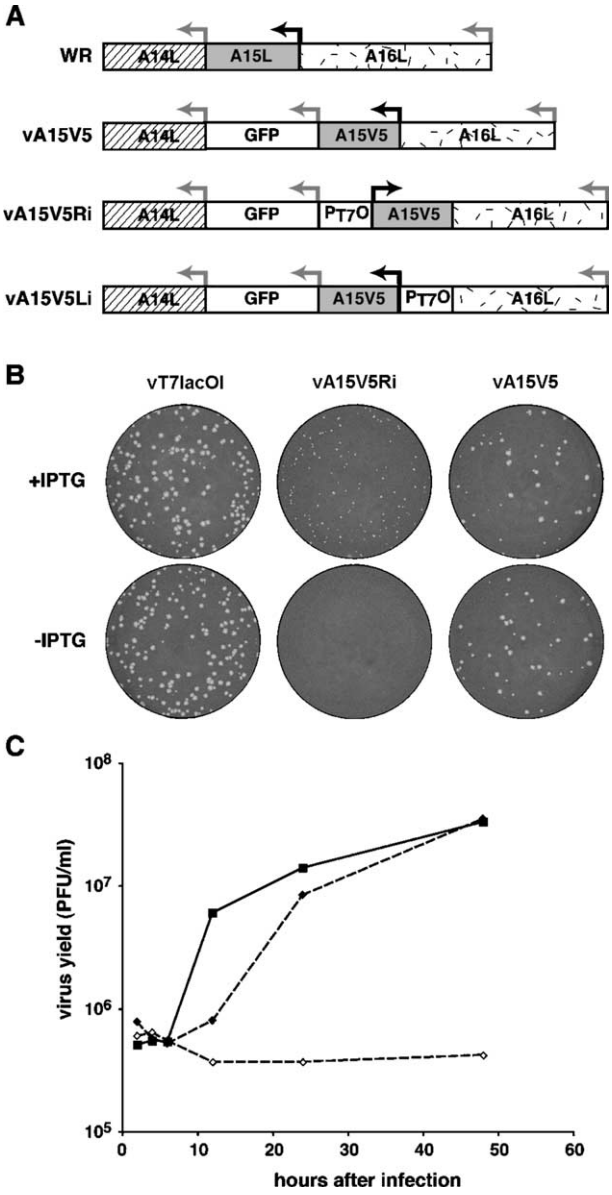

Fig. 6. Construction and characterization of vA15V5 inducible mutants. (A) Diagrams of portions of the VAC WR, vA15V5, vA15V5Ri, and vA15V5Li genomes. Abbreviation: GFP, enhanced green fluorescent protein; $P_{T7}O$, bacteriophage T7 promoter regulated by the *lac* operator. (B) Virus plaques. BS-C-1 monolayers were infected with vT7lacOI, vA15V5Ri, or vA15V5, and covered with a methylcellulose overlay. After 48 h, the overlay was removed and the plates were stained with crystal violet. (C) Time course of vA15V5Ri reproduction. BS-C-1 cells were infected with 5 PFU per cell of vT7lacOI (■) or vA15V5Ri in the presence (◆) or absence (◇) of 50 μM IPTG. Virus yields were determined at various times by plaque assay in the presence of IPTG.

at 25–50 μM (data not shown). In the absence of IPTG, the yield of vA15V5Ri was about 2 logs lower than the parental vT7lacOI. Even with an optimal concentration of IPTG, however, the kinetics of vA15V5Ri replication was retarded compared to vT7LacOI (Fig. 6C), consistent with the smaller plaque size.

Functional interaction between A15 and F10 kinase

Lysates of vA15V5Ri-infected cells were analyzed by SDS-PAGE followed by Western blotting using an anti-V5 MAb to correlate levels of A15V5 protein with virus replication. In the absence of IPTG, the A15V5 band was not seen even after 24 h (Fig. 7). The band was barely detectable at 5 and 10 μM IPTG, and was maximally induced at 50 μM. A time course experiment indicated that the onset of A15V5 synthesis under the inducible T7 promoter was slightly retarded relative to that of the natural promoter (data not shown). This delay could contribute to the lag in virus replication and the small plaque size.

In a previous study, we showed that the A17 membrane protein was stable in the absence of A30 or G7 expression but that phosphorylation of tyrosine and threonine residues was reduced, and that this effect was correlated with a decrease in the stability of the F10 protein kinase. To determine whether inhibition of A15 had similar effects on F10 and the phosphorylation of A17, lysates of cells infected with vA15V5Ri in the presence of increasing concentrations of IPTG were analyzed by SDS-PAGE followed by Western blotting with antibodies that recognize F10 and phosphorylated tyrosine and threonine in A17. The level of F10 and the tyrosine phosphorylation of A17 paralleled the induction of A15V5, suggesting that the kinase is unstable in the absence of A15 (Fig. 7).

Processing of viral core proteins and association of viral membranes and viroplasm are inhibited in the absence of A15V5 expression

Maturation of IV into IMV is coupled to the proteolytic cleavage of the viral precursor proteins P4a, P4b, and 28 K to generate the major core proteins 4a, 4b, and 25 K (Katz and Moss, 1970). Consequently, cleavage is inhibited when either A30 or G7 is repressed (Szajner et al., 2001b, 2003). To investigate the effect of inhibition of A15 expression on

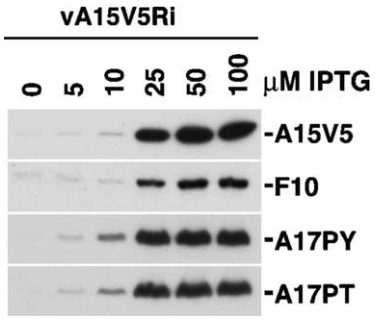

Fig. 7. Physical and functional dependence of F10 on A15V5 expression. Cells were infected with vA15V5Ri in the presence of indicated amounts of IPTG. After 24 h, cell lysates were examined by Western blotting with antibodies to V5, F10, tyrosine phosphates (PY), and threonine phosphates (PT).

the proteolytic processing of core proteins, we carried out pulse-chase experiments. Cells were infected with either vA15V5Ri in the presence or absence of IPTG. As a control, cells were infected with vT7LacOI in the presence or absence of rifampin, which blocks morphogenesis and proteolytic processing (Katz and Moss, 1970; Moss et al., 1969; Nagayama et al., 1970). Pulse labeling indicated that the core protein precursors P4a, P4b, and 28K were synthesized at similar levels in cells infected with different viruses under permissive or nonpermissive conditions (Fig. 8). However, proteolytic processing of P4a and 28K to the core proteins 4a and 25K was severely inhibited in the absence of A15 expression while cleavage of P4b was incompletely blocked (Fig. 8).

Electron microscopy was used to determine the effect of inhibition of A15 expression on the morphogenesis of VAC. Cells infected in the presence of IPTG contained large numbers of immature (Fig. 9B) and mature (not shown) virions, which were indistinguishable from those observed in cells infected with wild-type virus. In contrast, no mature virions were found in cells infected with vA15V5Ri in the absence of the inducer. Instead, there were large masses of dense viroplasm and most of the circular IV did not enclose electron-dense material that is normally observed in IV (Fig. 9A). Some viral membranes formed layers that closely resembled those seen in cells infected with vA30Li or vG7Li under nonpermissive conditions (Szajner et al., 2001b, 2003). Only a small minority of the IV made in the presence of IPTG appeared empty and masses of viroplasm were not seen (Fig. 9B).

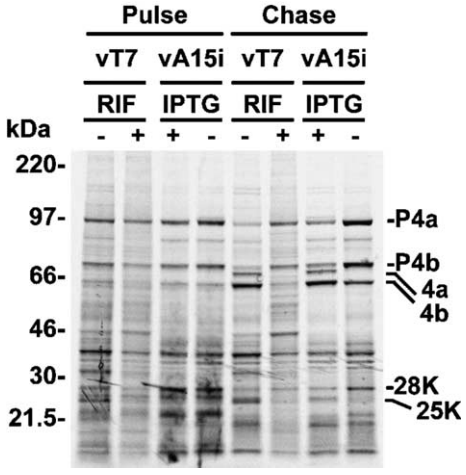

Fig. 8. Effect of A15V5 expression on the processing of viral proteins. Cells were infected with 5 PFU per cell of vA15V5Ri in the presence or absence of IPTG or the parent virus vT7lacOI in the presence or absence of rifampin (RIF). At 9 h after infection, the cells were pulse labeled with [^{35}S]methionine and cysteine for 30 min, washed, and chased for 13 h in medium containing excess unlabeled methionine and cysteine. The proteins were analyzed by SDS-PAGE and autoradiographs are shown. The masses in kDa are indicated on the left and the prominent precursor proteins P4a, P4b, and 28K and their major cleavage products 4a, 4b, and 25K, respectively, on the right.

Associations of viral membranes and viroplasm are dependent on D2 and D3

In a previous study, Dyster and Niles (1991) showed that proteolytic cleavage of the major core precursor protein P4a was impaired in cells infected at 40 °C with temperature-sensitive (ts) viruses that map to the D3R or D2L ORF, whereas processing of P4b was less affected. This is similar to the result we found by repressing A15 synthesis. To determine the step at which virion assembly was blocked, BSC-1 cells were infected with ts mutants Ets52 or Cts35, which map to D2L and D3R, respectively, at 31 or 40 °C for 20 h and analyzed by transmission electron microscopy. All viral structures, including crescents, IV, IMV, IEV, and CEV were observed in cells infected with Cts35 (Fig. 10B) or Ets52 (Fig. 10D) virus at 31 °C. In contrast, no mature virions were seen in cells infected with either ts virus at nonpermissive temperature. Instead, these cells showed large areas of cytoplasm devoid of cellular organelles (Figs. 10A and C), similar to the large cleared areas observed in cells infected with ts viruses that map to the F10L ORF. Some of these areas contained a small number of crescent-shaped and circular viral membranes, the majority of which lacked the electron-dense material that is normally enclosed by IV (Figs. 10A and C). In addition, large masses of electron-dense material with a lacey appearance and clearly separated from the viral membranes were observed (Fig. 10C).

We previously noticed that elevated temperature can have secondary effects on morphogenesis (Szajner et al., 2001a, 2004b), making it desirable to construct inducible mutants of D2 and D3. The partially overlapping arrangement of genes in the *Hin*dIII D fragment made it difficult to design inducible viruses by engineering the endogenous copies of D2 and D3 as we did with A15. We therefore depended on a two-step procedure in which the inducible copy is inserted in the hemagglutinin locus of vT7lacOI and the original copy is deleted (Szajner et al., 2001b). Recombinant VACs vD2Fli (Fig. 11A) and vD3Vgi (not shown), containing an IPTG-inducible copy of a Flag epitope-tagged D2 or vesicular stomatitis virus glycoprotein epitope-tagged D3, respectively, were constructed. Recombinant vD2Fli exhibited a severe defect in plaque formation in the absence of IPTG (Fig. 11B), whereas vD3Vgi was less affected (not shown) and was judged too leaky for use. Even in the presence of IPTG, the plaques formed by vD2Fli were small (Fig. 11B). Raising the IPTG above 25 μM IPTG had little effect (data not shown). Smaller than normal size plaques were also observed in cells infected with vD2Fl (Fig. 11B), which contains a C-terminal Flag-tagged copy of D2 under the D2 promoter, suggesting that the tag is deleterious to optimal viral replication or spread. Importantly, in a one-step growth experiment, the yield of vD2Fli in the absence of IPTG was nearly 2 logs lower than in the presence of inducer, indicating a specific requirement for D2Fl expression (Fig. 11C).

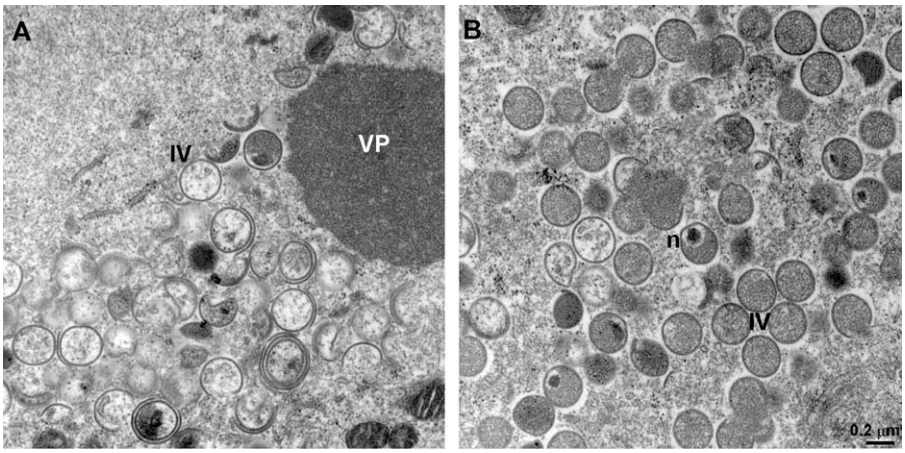

Fig. 9. Transmission electron microscopic images of cells infected with vA15V5Ri. BS-C-1 cells were infected with vA15V5Ri in the absence (A) or presence (B) of 50 μM IPTG. After 20 h, the cells were prepared for transmission electron microscopy. Electron micrographs are shown with the scale indicated by the bar. Abbreviations; VP, viroplasm; IV, immature virions; n, nucleoid within an IV.

To determine whether repression of D2 inhibited proteolytic cleavage of the major core proteins, BS-C-1 cells were infected with the vD2Fli virus in the presence or absence of IPTG and pulse labeled with a mixture of [^{35}S]methionine and [^{35}S]cysteine. As a control, cells were infected with vT7LacOI in the presence or absence of rifampin. The results were virtually identical to that shown in Fig. 8 for repression of A15V5. Inhibition of D2 expression had no effect on the synthesis of viral late proteins but reduced the formation of 4a and 25 K and to a lesser extent 4b (data not shown).

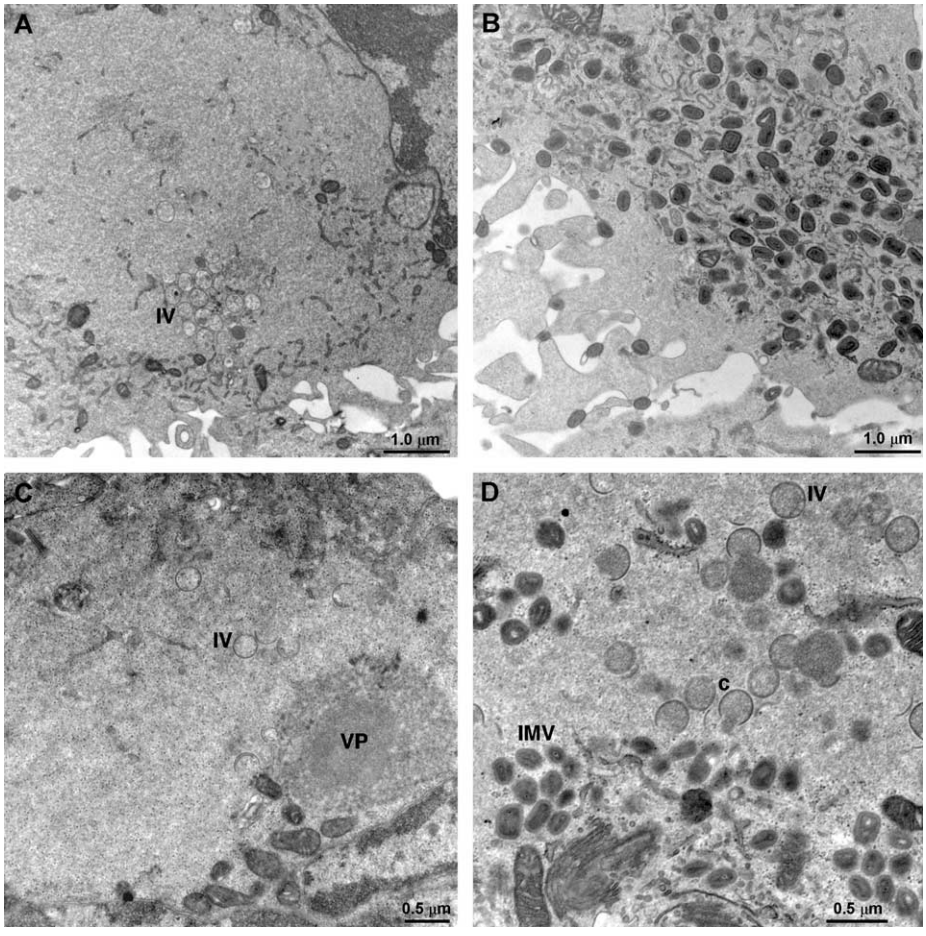

Fig. 10. Transmission electron microscopic images of cells infected with ts mutants that map to the D2L and D3R ORFs. BS-C-1 cells were infected with Ets52 (D2 mutant) at 40 °C (A) or 31 °C (B) or with Cts35 (D3 mutant) at 40 °C (C) or 31 °C (D). Abbreviations as in legend of Fig. 9.

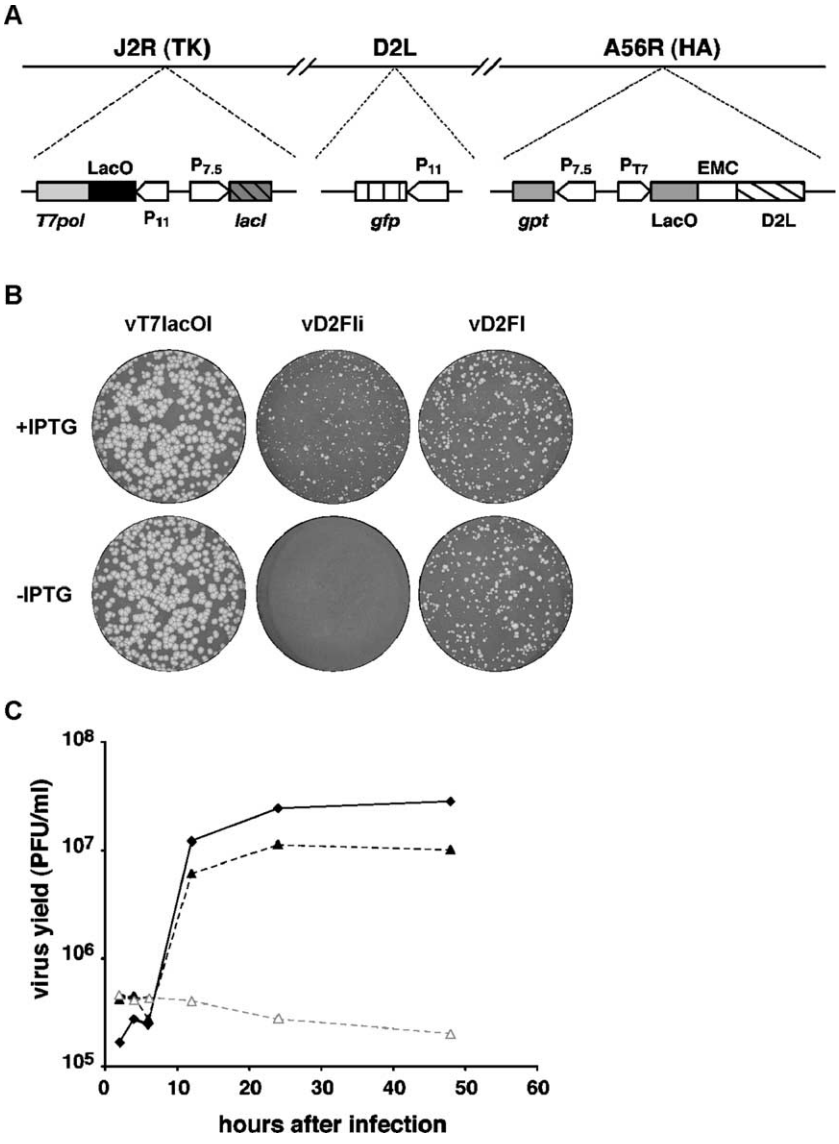

Fig. 11. Construction of an inducible D2 mutant. (A) Diagram of vD2Fli. The J2R (thymidine kinase, TK), D2L, and A56R (HA) loci are shown. Insertions into these loci are displayed below the line. Additional abbreviations: P_{11}, VAC late promoter; $P_{7.5}$, VAC early late promoter; LacO, *E. coli lac* operator; *lacI*, *E. coli lac* repressor gene; *T7 pol*, bacteriophage T7 RNA polymerase gene; P_{T7}, bacteriophage T7 promoter; EMC, encephalomyocarditis virus cap-independent translation enhancer element; *gfp*, enhanced green fluorescent protein gene; *gpt*, *E. coli* guanine phosphoribosyltransferase gene. (B) Effect of IPTG on plaque formation. BS-C-1 cells were infected with vT7lacOI, vD2Fli, or vD2Fl in the presence or absence of 50 μM IPTG. After 48 h, cell monolayers were stained with crystal violet. (C) Time course of vD2Fli replication in the presence or absence of IPTG. Cells were infected with vT7lacOI (◆) or vD2Fli in the presence (▲) or absence (Δ) of 50 μM IPTG. After 24 h, the cells were harvested and tittered on BS-C-1 cells in the presence of 50 μM IPTG.

Electron microscopy was used to determine whether inhibition of D2 expression resulted in a block in morphogenesis similar to the one observed in cells infected at the nonpermissive temperature with ts mutants. In these experiments, BSC-1 cells infected with vD2Fli at 37 °C in the presence or absence of IPTG were fixed at 20 h after infection and prepared for transmission electron microscopy. All forms of VAC, including crescents, IV, IMV, IEV, EEV, and CEV were readily found in cells infected with vD2Fli in the presence of IPTG (Fig. 12B and data not shown). In contrast, the cytoplasm of cells infected in the absence of the inducer showed no mature virions. Instead, these cells contained large masses of electron-dense viroplasm separated from large numbers of crescent-shaped and "empty" circular viral membranes (Fig. 12A). These structures are strikingly similar to those observed in cells infected with the inducible A30 (Szajner et al., 2001b), G7 (Szajner et al., 2003), J1 (Chiu and Chang, 2002), and A15 (this paper) mutants.

Discussion

The assembly of VAC virions involves interacting protein complexes. There is indirect evidence for a complex comprised of at least six proteins involved in transcription and mRNA processing that is targeted to virus cores by

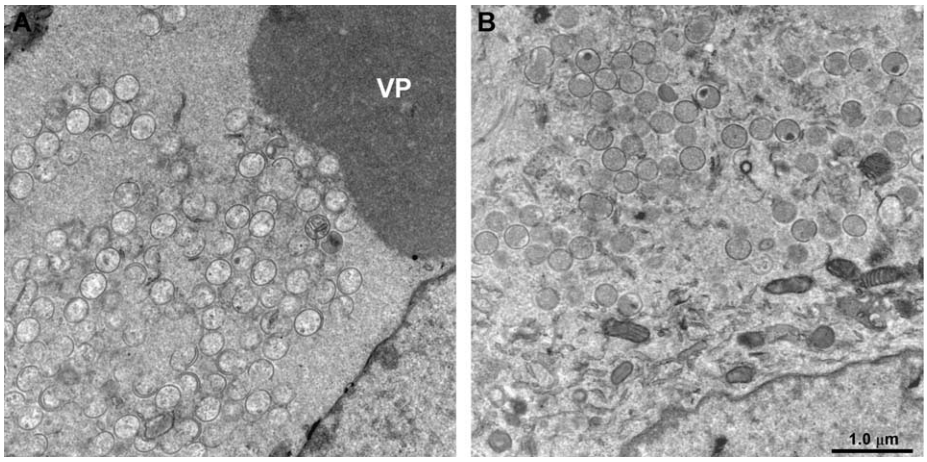

Fig. 12. Transmission electron microscopy of cells infected with vD2Fli in the absence (A) or presence (B) of IPTG. Procedures and abbreviations as in the legend of Fig. 9.

RAP94, an RNA polymerase specificity factor (Zhang et al., 1994). In addition, there are numerous examples of pair-wise protein interactions. Here we describe a complex comprised of seven proteins that are involved in an early stage of morphogenesis. The F10 protein kinase was selected as the target for our study because of previous evidence that it is required for assembly of viral membranes (Traktman et al., 1995; Wang and Shuman, 1995) and interacts with two proteins, A30 and G7, which are required for association of viral membranes with viroplasm (Szajner et al., 2001b, 2003, 2004b). To isolate the putative complex, we infected cells with a recombinant VAC in which the F10 protein had a short C-terminal epitope-tag. As a control, cells were infected with wild-type VAC lacking the tag. By subjecting the extracts from both infections to an identical immunoaffinity purification procedure with a MAb to the epitope tag, we distinguished specific and nonspecific binding proteins. The specific bands were excised from a denaturing gel and tryptic peptides from seven viral proteins, namely A15, A30, D2, D3, F10, G7, and J1, were identified by liquid chromatography and mass spectroscopy. At this stage, we could not be sure whether the isolated proteins interacted individually or as part of a large complex with F10. Evidence for the latter was obtained by epitope tagging A15, D2, and D3 separately and in each case affinity purifying the same set of proteins. We suspect that there is little free F10, A30, or G7 because these proteins are unstable in the absence of other components of the complex. It will surely be interesting to determine the mechanism of degradation of the uncomplexed proteins. In this context, Dyster and Niles (1991) found that a ts mutation of D2 rendered both D2 and D3 unstable and that a ts mutation of D3 rendered both proteins unstable. Except for F10 and J1, the polypeptides comprising the complex appeared to be present in equimolar ratios. F10 appears to be present in only a subset of complexes and J1 might be present as a homodimer.

A high-throughput yeast two-hybrid analysis revealed 37 VAC protein interactions, but the only one relevant to the present study was the interaction of J1 with itself (McCraith et al., 2000). Nevertheless, this system might identify additional interactions if protein fragments of specific proteins were used. Another approach, consisting of the expression pairs of proteins in a cell-free system, suggested an interaction of D2 and D3 and of D2 and A15 (P.S., unpublished observation).

The seven proteins forming the complex are conserved in all chordopoxviruses, implying a common function in each. However, none of the proteins except for F10 have any recognizable motifs, pointing to purely structural roles. Indeed, repression of A30, G7, J1, A15, or D2 gives the same phenotype: the failure of viral membranes and viroplasm to associate with each other. Present and previous studies have shown that A15, A30, D2, D3, F10, and G7 are localized in virus cores (Dyster and Niles, 1991; Szajner et al., 2001b, 2003, 2004b). Although J1 was reported to be a membrane protein (Chiu and Chang, 2002), we found it to be associated with viroplasm and cores (P.S and A.S.W., unpublished). Nevertheless, it seems likely that the protein complex interacts with some membrane protein(s) to accomplish its role in morphogenesis. The A17 and A14 membrane proteins are good candidates, as they are phosphorylated by the F10 protein kinase (Betakova et al., 1999; Derrien et al., 1999; Mercer and Traktman, 2003; Traktman et al., 2000). The interaction between the complex and membrane proteins may not withstand the conditions of cell lysis and immunopurification, making alternative methods of investigation necessary.

Materials and methods

Cell and viruses

BS-C-1 (ATCC CCL6) and HeLa S3 (ATCC CCL2.2) cells were grown in Eagle's minimal essential medium (E-MEM) and Dulbecco's modified Eagle's medium (D-MEM),

respectively, each obtained from Quality Biologicals Inc and supplemented with 10% fetal bovine serum (FBS). Wild-type and recombinant VACs were propagated in HeLa cells as previously described (Earl et al., 1998a). Conditional lethal inducible viruses were propagated in the presence of 50 μM isopropyl-β-D-thiogalactopyranoside (IPTG) and 2.5% FBS. All virus stocks were stored at −70 °C.

Construction of recombinant viruses

Standard procedures were used for construction and isolation of recombinant viruses (Earl et al., 1998b) with modifications (Szajner et al., 2004b). Plaques containing recombinant VACs expressing GFP were picked using an inverted fluorescence microscope and clonally purified by repeated plaque isolations. Inserted genes were analyzed by PCR and DNA sequencing.

Plaque assay

BS-C-1 cell monolayers, in 6-well tissue culture plates, were infected with 10-fold serial dilutions of virus. After 1 h of adsorption, inocula were removed and replaced with complete E-MEM containing 2.5% FBS, 0.5% methylcellulose, with or without 50 μM IPTG. The infected cells were incubated at 37 °C for 2 days, stained with crystal violet, and the plaques counted (Earl et al., 1998b).

One-step virus growth

BS-C-1 cell monolayers, in 6-well tissue culture plates, were infected with 5 PFU of VAC per cell. After 1 h, inocula were removed and cell monolayers were washed twice with E-MEM containing 2.5% FBS. The cells were then incubated in E-MEM containing 2.5% FBS with or without 50 μM IPTG and harvested at various times after infection. The infected cells were subjected to three freeze/thaw cycles, sonicated, and stored at −70 °C. Virus titers were determined by plaque assay in the presence of 50 μM IPTG.

Antibodies

The murine MAb anti-V5 (Invitrogen, Carlsbad, CA) recognizes the 14-amino acid sequence GKPIPNPLLGLDST found in the P and V proteins of the paramyxovirus SV5. The murine MAb anti-FLAG M2 (Sigma-Aldrich, St Louis, MO) recognizes the 9-amino acid sequence DYKDDDDK. Rabbit polyclonal anti-phosphotyrosine (anti-pTyr) and anti-phosphothreonine (anti-pThr) antiserum was purchased from Zymed Laboratories (South San Francisco, CA).

Affinity purification and mass spectroscopy of protein complexes

Three roller bottles containing 4.5×10^8 BS-C-1 cells were infected with vF10V5 at a multiplicity of 3 PFU per cell for 2 h and incubated at 37 °C. At 48 h after infection, the cells were harvested, washed with cold Tris-buffered saline, and lysed in the presence of protease inhibitor cocktail tablets for 30 min on ice. The cell lysate was clarified by centrifugation at 20,000 × *g* for 30 min at 4 °C and the supernatant was rotated with 1 ml of 50% vol/vol slurry of the anti-V5 affinity matrix for 4 h. The beads were washed five times with 10 ml of lysis buffer. The proteins were eluted by washing the beads two times with 0.5 ml of 100 mM glycine pH 2.0. The eluted proteins were precipitated with 20% trichloroacetic acid, resuspended in 1 M Tris pH 9.0 plus 2× sample buffer and analyzed by SDS-PAGE, and visualized by Coomassie blue staining. Coomassie blue-stained bands were excised and subjected to in-gel tryptic digestion (Moritz et al., 1995). The resulting digests were concentrated and analyzed by capillary high pressure liquid chromatography coupled to a Model LCQ ion trap mass spectrometer (ThermoFinnigan, San Jose, CA) equipped with an electrospray interface as described (Szajner et al., 2003). Uninterpreted MS/MS spectra were searched against the NR database utilizing BioWorks and SEQUEST software (ThermoFinnigan).

Western blot analysis

Proteins from infected cell lysates or purified virions were resolved by SDS- PAGE and electrophoretically transferred to a nitrocellulose membrane (Osmonics, Inc). Membrane blocking, antibody binding, and chemiluminescent detection were carried out as previously described (Szajner et al., 2004b).

Virion fractionation

Purified virus particles (10^8 PFU) were incubated in a reaction mixture containing 50 mM Tris–HCl pH 7.5, 1% (vol/vol) NP40, with or without 50 mM dithiothreitol for 1 h at 37 °C. Insoluble and soluble materials were separated by centrifugation at 20,000 × *g* for 30 min at 4 °C.

Electron microscopy

Infected cells were fixed in 2% glutaraldehyde in 0.1 M sodium cacodylate buffer, washed in 0.1 M sodium cacodylate buffer, post-fixed with reduced osmium tetroxide, and washed in buffer. Cells were dehydrated in a series of ethyl alcohol dilutions (50%, 70%, and 100%) followed by incubation in propylene oxide. The cells were then embedded in EMbed 812. Sections were obtained using the Leica Ultracut S ultramicrotome. Thin sections were stained with 7% uranyl acetate in 50% ethanol and then with 0.01% lead citrate and analyzed on the Philips CM100 transmission electron microscope.

Analysis of metabolically labeled polypeptides by SDS-PAGE

BS-C-1 cells were infected with 10 PFU of virus per cell and incubated for 1 h at 37 °C. The inocula were removed and the infected cells were incubated with E-MEM containing 2.5% FBS, with or without of 50 μM IPTG or with or without 100 μg/ml of rifampin. At 9 h after infection, pulse labeling was carried out with 100 μCi/ml of [^{35}S]methionine and [^{35}S]cysteine for 30 min in methionine- and cysteine-free medium containing 2.5% dialyzed FBS. The cells were harvested, washed once with cold phosphate-buffered saline, and incubated with 0.01 μg/μl of micrococcal nuclease in 10 mM Tris–HCl pH 7.5, 10 mM KCl, 1 mM $CaCl_2$, 0.2% (vol/vol) NP-40, 20 mM β-mercaptoethanol, and 0.2 mM phenylmethylsulfonyl fluoride for 30 min on ice. For pulse chase experiments, the labeling medium was removed and replaced with E-MEM containing 2.5% FBS and incubated for 15 h prior to lysis. The samples were analyzed by SDS-PAGE as previously described (Szajner et al., 2004b).

Acknowledgments

We thank Wen Chang for antibody to J1 and Norman Cooper for cells.

References

Alexander, W.A., Moss, B., Fuerst, T.R., 1992. Regulated expression of foreign genes in vaccinia virus under the control of bacteriophage T7 RNA polymerase and the *Escherichia coli lac* repressor. J. Virol. 66, 2934–2942.

Ansarah-Sobrinho, C., Moss, B., 2004. Role of the I7 protein in proteolytic processing of vaccinia virus membrane and core components. J. Virol. 78, 6335–6343.

Appleyard, G., Hapel, A.J., Boulter, E.A., 1971. An antigenic difference between intracellular and extracellular rabbitpox virus. J. Gen. Virol. 13, 9–17.

Betakova, T., Wolffe, E.J., Moss, B., 1999. Regulation of vaccinia virus morphogenesis: phosphorylation of the A14L and A17L membrane proteins and C-terminal truncation of the A17L protein are dependent on the F10L protein kinase. J. Virol. 73, 3534–3543.

Betakova, T., Wolffe, E.J., Moss, B., 2000. Vaccinia virus A14.5L gene encodes a hydrophobic 53-amino acid virion membrane protein that enhances virulence in mice and is conserved amongst vertebrate poxviruses. J. Virol. 74, 4085–4092.

Blasco, R., Moss, B., 1992. Role of cell-associated enveloped vaccinia virus in cell-to-cell spread. J. Virol. 66, 4170–4179.

Blasco, R., Sisler, J.R., Moss, B., 1993. Dissociation of progeny vaccinia virus from the cell membrane is regulated by a viral envelope glycoprotein: effect of a point mutation in the lectin homology domain of the A34R gene. J. Virol. 67, 3319–3325.

Boulter, E.A., Appleyard, G., 1973. Differences between extracellular and intracellular forms of poxvirus and their implications. Prog. Med. Virol. 16, 86–108.

Byrd, C.M., Bolken, T.C., Hruby, D.E., 2003. Molecular dissection of the vaccinia virus I7L core protein proteinase. J. Virol. 77, 11279–11283.

Chiu, W.L., Chang, W., 2002. Vaccinia virus J1R protein: a viral membrane protein that is essential for virion morphogenesis. J. Virol. 76, 9575–9587.

Dales, S., Siminovitch, L., 1961. The development of vaccinia virus in Earle's L strain cells as examined by electron microscopy. J. Biophys. Biochem. Cytol. 10, 475–503.

Derrien, M., Punjabi, A., Khanna, R., Grubisha, O., Traktman, P., 1999. Tyrosine phosphorylation of A17 during vaccinia virus infection: involvement of the H1 phosphatase and the F10 kinase. J. Virol. 73, 7287–7296.

Dyster, L.M., Niles, E.G., 1991. Genetic and biochemical characterization of vaccinia virus genes D2L and D3R which encode virion structural proteins. Virology 182, 455–467.

Earl, P.L., Cooper, N., Wyatt, S., Moss, B., Carroll, M.W., 1998a. Preparation of cell cultures and vaccinia virus stocks. In: Ausubel, F.M., Brent, R., Kingston, R.E., Moore, D.D., Seidman, J.G., Smith, J.A., Struhl, K. (Eds.), Current Protocols in Molecular Biology. John Wiley & Sons, New York, pp. 16.16.1–16.16.3.

Earl, P.L., Moss, B., Wyatt, L.S., Carroll, M.W., 1998b. Generation of recombinant vaccinia viruses. In: Ausubel, F.M., Brent, R., Kingston, R.E., Moore, D.D., Seidman, J.G., Smith, J.A., Struhl, K. (Eds.), Current Protocols in Molecular Biology. Greene Publishing Associates and Wiley Interscience, New York, pp. 16.17.1–16.17.19.

Fuerst, T.R., Niles, E.G., Studier, F.W., Moss, B., 1986. Eukaryotic transient-expression system based on recombinant vaccinia virus that synthesizes bacteriophage T7 RNA polymerase. Proc. Natl. Acad. Sci. U.S.A. 83, 8122–8126.

Geada, M.M., Galindo, I., Lorenzo, M.M., Perdiguero, B., Blasco, R., 2001. Movements of vaccinia virus intracellular enveloped virions with GFP tagged to the F13L envelope protein. J. Gen. Virol. 82, 2747–2760.

Grimley, P.M., Rosenblum, E.N., Mims, S.J., Moss, B., 1970. Interruption by rifampin of an early stage in vaccinia virus morphogenesis: accumulation of membranes which are precursors of virus envelopes. J. Virol. 6, 519–533.

Hiller, G., Weber, K., 1985. Golgi-derived membranes that contain an acylated viral polypeptide are used for vaccinia virus envelopment. J. Virol. 55, 651–659.

Hollinshead, M., Rodger, G., Van Eijl, H., Law, M., Hollinshead, R., Vaux, D.J., Smith, G.L., 2001. Vaccinia virus utilizes microtubules for movement to the cell surface. J. Cell Biol. 154, 389–402.

Katz, E., Moss, B., 1970. Formation of a vaccinia virus structural polypeptide from a higher molecular weight precursor: inhibition by rifampicin. Proc. Natl. Acad. Sci. U.S.A. 6, 677–684.

McCraith, S., Holtzman, T., Moss, B., Fields, S., 2000. Genome-wide analysis of vaccinia virus protein–protein interactions. Proc. Natl. Acad. Sci. U.S.A. 97, 4879–4884.

Mercer, J., Traktman, P., 2003. Investigation of structural and functional motifs within the vaccinia virus A14 phosphoprotein, an essential component of the virion membrane. J. Virol. 77, 8857–8871.

Moritz, R., Eddes, J., Hong, J., Reid, G., Simpson, R., 1995. Rapid separation of proteins and peptides using conventional silica-based supports: identification of 20 gel proteins following in-gel proteolysis. In: Crabb, J.W. (Ed.), Techniques in Protein Chemistry. Academic Press, San Diego, pp. 311–319.

Moss, B., Rosenblum, E.N., 1973. Protein cleavage and poxvirus morphogenesis: tryptic peptide analysis of core precursors accumulated by blocking assembly with rifampicin. J. Mol. Biol. 81, 267–269.

Moss, B., Rosenblum, E.N., Katz, E., Grimley, P.M., 1969. Rifampicin: a specific inhibitor of vaccinia virus assembly. Nature 224, 1280–1284.

Nagayama, A., Pogo, B.G.T., Dales, S., 1970. Biogenesis of vaccinia: separation of early stages from maturation by means of rifampicin. Virology 40, 1039–1051.

Payne, L.G., 1980. Significance of extracellular virus in the in vitro and in vivo dissemination of vaccinia virus. J. Gen. Virol. 50, 89–100.

Rietdorf, J., Ploubidou, A., Reckmann, I., Holmström, A., Frischknecht, F., Zettl, M., Zimmerman, T., Way, M., 2001. Kinesin dependent move-

ment on microtubules precedes actin based motility of vaccinia virus. Nat. Cell Biol. 3, 992–1000.

Risco, C., Rodriguez, J.R., Lopez-Iglesias, C., Carrascosa, J.L., Esteban, M., Rodriguez, D., 2002. Endoplasmic reticulum-Golgi intermediate compartment membranes and vimentin filaments participate in vaccinia virus assembly. J. Virol. 76, 1839–1855.

Schmelz, M., Sodeik, B., Ericsson, M., Wolffe, E.J., Shida, H., Hiller, G., Griffiths, G., 1994. Assembly of vaccinia virus: the second wrapping cisterna is derived from the trans Golgi network. J. Virol. 68, 130–147.

Senkevich, T.G., White, C.L., Koonin, E.V., Moss, B., 2002. Complete pathway for protein disulfide bond formation encoded by poxviruses. Proc. Natl. Acad. Sci. U.S.A. 99, 6667–6672.

Stokes, G.V., 1976. High-voltage electron microscope study of the release of vaccinia virus from whole cells. J. Virol. 18, 636–643.

Szajner, P., Weisberg, A.S., Moss, B., 2001a. Unique temperature-sensitive defect in vaccinia virus morphogenesis maps to a single nucleotide substitution in the A30L gene. J. Virol. 75, 11222–11226.

Szajner, P., Weisberg, A.S., Wolffe, E.J., Moss, B., 2001b. Vaccinia virus A30L protein is required for association of viral membranes with dense viroplasm to form immature virions. J. Virol. 75, 5752–5761.

Szajner, P., Jaffe, H., Weisberg, A.S., Moss, B., 2003. Vaccinia virus G7L protein interacts with the A30L protein and is required for association of viral membranes with dense viroplasm to form immature virions. J. Virol. 77, 3418–3429.

Szajner, P., Weisberg, A.S., Moss, B., 2004a. Evidence for an essential catalytic role of the F10 protein kinase in a vaccinia virus morphogenesis. J. Virol. 78, 257–265.

Szajner, P., Weisberg, A.S., Moss, B., 2004b. Physical and functional interactions between vaccinia virus F10 protein kinase and virion assembly proteins A30 and G7. J. Virol. 78, 266–274.

Tooze, J., Hollinshead, M., Reis, B., Radsak, K., Kern, H., 1993. Progeny vaccinia and human cytomegalovirus particles utilize early endosomal cisternae for their envelopes. Eur. J. Cell Biol. 60, 163–178.

Traktman, P., Caligiuri, A., Jesty, S.A., Sankar, U., 1995. Temperature-sensitive mutants with lesions in the vaccinia virus F10 kinase undergo arrest at the earliest stage of morphogenesis. J. Virol. 69, 6581–6587.

Traktman, P., Liu, K., DeMasi, J., Rollins, R., Jesty, S., Unger, B., 2000. Elucidating the essential role of the A14 phosphoprotein in vaccinia virus morphogenesis: construction and characterization of a tetracycline-inducible recombinant. J. Virol. 74, 3682–3695.

Wang, S., Shuman, S., 1995. Vaccinia virus morphogenesis is blocked by temperature-sensitive mutations in the F10 gene, which encodes protein kinase 2. J. Virol. 69, 6376–6388.

Ward, B.M., Moss, B., 2001a. Vaccinia virus intracellular movement is associated with microtubules and independent of actin tails. J. Virol. 75, 11651–11663.

Ward, B.M., Moss, B., 2001b. Visualization of intracellular movement of vaccinia virus virions containing a green fluorescent protein-B5R membrane protein chimera. J. Virol. 75, 4802–4813.

Ward, B.M., Moss, B., 2004. Vaccinia virus A36R membrane protein provides a direct link between intracellular enveloped virions and the microtubule motor kinesin. J. Virol. 78, 2486–2493.

Zhang, Y., Ahn, B.-Y., Moss, B., 1994. Targeting of a multicomponent transcription apparatus into assembling vaccinia virus particles requires RAP94, an RNA polymerase-associated protein. J. Virol. 68, 1360–1370.